

# Ocean optics estimation for absorption, backscattering, and phase function parameters

Ammar H. Hakim and Norman J. McCormick

We propose and test an inverse ocean optics procedure with numerically simulated data for the determination of inherent optical properties using in-water radiance measurements. If data are available at only one depth within a deep homogeneous water layer, then the single-scattering albedo and the single parameter that characterizes the Henyey–Greenstein phase function can be estimated. If data are available at two depths, then these two parameters can be determined along with the optical thickness so that the absorption and scattering coefficients, and also the backscattering coefficient, can be estimated. With a knowledge of these parameters, the albedo and Lambertian fraction of reflected radiance of the bottom can be determined if measurements are made close to the bottom. A simplified method for determining the optical properties of the water also is developed for only three irradiance-type measurements if the radiance is approximately in the asymptotic regime. © 2003 Optical Society of America  
*OCIS codes:* 010.4450, 030.5620, 100.3190, 160.4760, 290.1350, 290.3200.

## 1. Introduction

The estimation of the inherent optical properties (IOPs) of ocean waters from apparent optical properties is a key step in the characterization of the primary productivity of ocean waters.<sup>1</sup> Knowledge of the absorption and backscattering coefficients,  $a$  and  $b_b$ , of natural waters can be used to determine the water constituents and abundances if measurements are made at multiple wavelengths. Although these two properties can be estimated from remote sensing measurements of ocean color, *in situ* algorithms also are of value for validation purposes.<sup>2–6</sup> Although there are instruments with which to determine the attenuation of light from a source passing directly through a water sample, we choose to use a procedure that utilizes the natural light within the water column. With this approach one could use an iterative approach and repetitively solve the radiative transfer equation (RTE) while searching to minimize a cost (typically a least-squares) function when determining optical properties.<sup>2,4,6</sup> However, in this paper we

computationally explore the potential of an analytic formulation in which measured radiance data are used without repetitive solutions of the RTE. Earlier research of this type has relied on use of upward and downward plane irradiance detectors,<sup>3</sup> or on use of downward plane irradiance measurements and either upward plane irradiance or vertically upward radiance measurements.<sup>5</sup>

Our procedure is one in which we must assume the validity of the one-parameter Henyey–Greenstein (HG) scattering phase function model<sup>7</sup> to minimize the number of unknowns that describe the scattering. Although this phase function does not perfectly match the particle phase function typically used to model case 1 open waters,<sup>1,8</sup> the exact shape of the phase function is not as important as the correct value of the backscattering fraction.<sup>9</sup> The HG model also has been used by Chalhoub and Campos Velho<sup>6</sup> who restricted their attention to estimating the single-scattering albedo and the HG parameter from plane irradiance and also scalar irradiance measurements, which are more difficult to make than the remote sensing reflectance measurements relied on by Leathers *et al.*<sup>5</sup>

The general method proposed here requires that radiance measurements in multiple directions be made. Radiance measurements are difficult to make in a water column, admittedly, although prototype instruments have been developed by Voss and co-workers.<sup>10–13</sup> Thus, although our approach has the potential to obtain more parameters that charac-

---

A. H. Hakim (ahakim@u.washington.edu) and N. J. McCormick (mccor@u.washington.edu) are with the Department of Mechanical Engineering, Box 352600, University of Washington, Seattle, Washington 98195-2600.

Received 20 May 2002; revised manuscript received 4 November 2002.

0003-6935/03/060931-08\$15.00/0

© 2003 Optical Society of America

terize the water than other procedures,<sup>5,6</sup> we must admit that without a good set of experimental data we can only numerically predict the possible performance of our procedure when used in actual experiments.

With an appropriate set of radiance data that is symmetric with respect to the azimuthal angle, or has been averaged about that angle, we are proposing our procedure for two possible applications. If the water column is deep and measurements are being made at only one depth, then we can determine the single-scattering albedo  $\varpi$  and the single parameter  $g$  that characterizes the HG phase function. If radiance measurements are available at two known depths in the water, then the optical thickness  $\Delta\tau$  between the two positions also can be estimated; from this the beam attenuation coefficient  $c = a + b$  can be determined, where  $a$  is the absorption coefficient and  $b$  is the scattering coefficient. The values of  $\varpi = b/c$  and  $c$  then give  $a$  and  $b$ , and then  $b$  and  $g$  give the backscattering coefficient  $b_b$ .

After the values of  $\varpi$  and  $g$  have been obtained, the bottom albedo  $\rho$  and Lambertian fraction  $\gamma$  corresponding to a combined Lambertian–specular reflection model can be obtained if data from one of the two (or additional) radiance measurements are from close to the bottom. Our proposed method for determining  $\rho$  differs from one that relies on the assumption that the radiance is approximately asymptotic near the bottom.<sup>14</sup>

Siewert<sup>15</sup> has used a portion of this procedure to make preliminary tests of the equations for determining  $\varpi$ ,  $g$ , and  $\Delta\tau$  in simple test problems in which he assumed the HG phase function for all his tests. Here we test the procedure with calculations from Hydrolight<sup>8</sup> that simulate open ocean waters and develop a procedure to also determine  $a$ ,  $b_b$ ,  $\rho$ , and  $\gamma$ .

In Sections 2 and 3 we test our procedure with radiance measurements. Then in Section 4 we develop an approximate method with which to determine  $\varpi$  and  $g$ . The beauty of the approximate method is that data from only three irradiance-type measurements are needed: the scalar irradiance and planar irradiance and a third irradiance measured by Doss and Wells.<sup>16</sup> But this simplified approach does come with the penalty that the results are not as accurate as those from radiance measurements when data are taken near the surface. Numerical results with the approximate method are obtained in Section 5, followed by a discussion of all the results in Section 6.

## 2. General Equations

We are interested in the azimuthally averaged radiance  $L(z, \mu)$  (in units of  $\text{W m}^{-2} \text{sr}^{-1} \text{nm}^{-1}$ ) that satisfies the integrodifferential RTE<sup>1</sup>:

$$\mu \frac{\partial L(z, \mu)}{\partial z} + cL(z, \mu) = b \int_{-1}^1 \tilde{\beta}(\mu, \mu') L(z, \mu') d\mu', \quad 0 \leq z \leq z_*, \quad (1)$$

where  $\tilde{\beta}$  is the scattering phase function normalized such that  $\int_{-1}^1 \tilde{\beta}(\mu, 1) d\mu = 1$ ,  $\mu$  is the cosine of the polar angle with respect to the downward depth  $z$  in meters, and  $z_*$  is the depth of the water column. All quantities in Eq. (1) are implicitly a function of a single wavelength. The backscattering coefficient  $b_b$  is related to  $b$  by

$$\frac{b_b}{b} = \int_{-1}^0 \tilde{\beta}(\mu, 1) d\mu. \quad (2)$$

The scattering phase function in Eq. (1) can be expanded in Legendre polynomials, yielding

$$\tilde{\beta}(\mu, \mu') = \frac{1}{2} \sum_{n=0}^N (2n+1) f_n P_n(\mu) P_n(\mu'), \quad f_0 = 1, \quad (3)$$

where  $f_n$  are the expansion coefficients,  $P_n(\mu)$  are the Legendre polynomials, and  $N$  is the assumed maximum degree of scattering anisotropy. The parameter  $f_1 \equiv g$  is the asymmetry factor for a single-scattering event. For the HG model,  $f_n = g^n$  and, in principle,  $N \rightarrow \infty$ . Combining Eqs. (1) and (3) and converting to distances measured in optical depths  $\tau$ , we obtain

$$\mu \frac{\partial L(\tau, \mu)}{\partial \tau} + L(\tau, \mu) = \frac{\varpi}{2} \sum_{n=0}^{\infty} (2n+1) g^n P_n(\mu) \times \int_{-1}^1 P_n(\mu') L(\tau, \mu') d\mu', \quad 0 \leq \tau \leq \tau_*, \quad (4)$$

where  $\tau_*$  is the optical depth of the water column.

### A. Determination of the Albedo and Mean Cosine of Scattering

Two general inverse equations were developed to estimate  $\varpi$  and the  $f_n$  coefficients from azimuthally dependent radiance measurements. With the specializing assumption of an azimuthally symmetric or azimuthally integrated radiance, the two equations to estimate  $\varpi$  and  $g$  for the HG phase functions by use of measured radiances at two arbitrary depths  $\tau = \tau_1$  and  $\tau_2$ ,  $0 \leq \tau_1 \leq \tau_2 \leq \tau_*$  are<sup>17</sup>

$$\varpi \sum_{n=0}^{\infty} (-1)^n (2n+1) g^n \{ [E_n(\tau_2)]^2 - E_n(\tau_1) \} = 4[S(\tau_2) - S(\tau_1)], \quad (5)$$

$$\varpi \sum_{n=0}^{\infty} (-1)^n (2n+1) \tilde{g}^n \{ [\tilde{E}_n(\tau_2)]^2 - [\tilde{E}_n(\tau_1)]^2 \} = 4[\tilde{S}(\tau_2) - \tilde{S}(\tau_1)], \quad (6)$$

where

$$E_n(\tau) = \int_{-1}^1 P_n(\mu) L(\tau, \mu) d\mu, \quad (7)$$

$$S(\tau) = \int_0^1 L(\tau, \mu) L(\tau, -\mu) d\mu, \quad (8)$$

$$\tilde{E}_n(\tau) = \int_{-1}^1 \mu P_n(\mu) L(\tau, \mu) d\mu, \quad (9)$$

$$\tilde{S}(\tau) = \int_0^1 \mu^2 L(\tau, \mu) L(\tau, -\mu) d\mu, \quad (10)$$

$$\tilde{g}^n = g^n / (1 - \varpi g^n). \quad (11)$$

The first step of our procedure is to iteratively solve nonlinear Eqs. (5) and (6) to determine  $g$  and  $\varpi$ . Radiance measurements at two depths  $\tau_1$  and  $\tau_2$  are required unless it is assumed that the water is so deep that  $L(\tau_*, \mu) = 0$  so that measurements at only  $\tau_1$  are needed. It should be noted that, if  $\tau_1$  occurs at an air-water interface, Eqs. (5) and (6) do not account for the index of refraction mismatch, which means that the estimated  $\varpi$  and  $g$  are more subject to errors if used with radiances near the surface. This is investigated in Section 3.

One can expand the radiance in the complete set of Legendre polynomials as

$$L(\tau, \mu) = 2^{-1} \sum_{n=0}^{\infty} (2n+1) E_n(\tau) P_n(\mu). \quad (12)$$

Use of this expansion in Eq. (8), followed by use of the Legendre polynomial orthogonality relation after converting the integral over  $[0, 1]$  to  $[-1, 1]$ , we obtain

$$S(\tau) = \sum_{n=0}^{\infty} (-1)^n (2n+1) E_n^2(\tau), \quad (13)$$

so Eq. (5) for the HG phase function can be written in a more succinct form:

$$\sum_{n=0}^{\infty} (-1)^n (2n+1) (1 - \varpi g^n) \{ [E_n(\tau_2)]^2 - E_n(\tau_1) \} = 0. \quad (14)$$

A similar analysis to evaluate  $\tilde{S}(\tau)$ , in which the Legendre polynomial recursion must be used, yields

$$\tilde{S}(\tau) = - \sum_{n=0}^{\infty} (-1)^n (2n+1) \tilde{E}_n^2(\tau), \quad (15)$$

so a shorter form for Eq. (6) for the HG phase function follows after use of Eq. (11):

$$\sum_{n=0}^{\infty} (-1)^n (2n+1) (1 - \varpi g^n)^{-1} \times \{ [\tilde{E}_n(\tau_2)]^2 - [\tilde{E}_n(\tau_1)]^2 \} = 0. \quad (16)$$

## B. Determination of the Absorption and Scattering Coefficients

To determine  $a$ ,  $b$ , and  $b_b$ , values of  $\varpi$  and  $g$  are needed from measurements of  $L(\tau, \mu)$  at two depths. This is done when we use Siewert's procedure to estimate  $c$  from<sup>15</sup>

$$c = (\tau_2 - \tau_1) / (z_2 - z_1). \quad (17)$$

He obtained the set of equations

$$\Delta\tau = \tau_2 - \tau_1 = \nu_j \ln [M(\tau_1, \nu_j) / M(\tau_2, \nu_j)], \quad (18)$$

$$j = 1 \text{ to } J,$$

any one of which can be used to determine  $\Delta\tau$ . Here

$$M(\tau, \nu_j) = \int_{-1}^1 \mu \phi(\nu_j, \mu) L(\tau, \mu) d\mu, \quad (19)$$

$$\phi(\nu_j, \mu) = \frac{\varpi \nu_j}{2} \sum_{n=0}^{\infty} (2n+1) g^n \frac{g_n(\nu_j) P_n(\mu)}{\nu_j - \mu}, \quad (20)$$

where the eigenvalues of the RTE can be computed as the roots  $\nu_j \notin [-1, 1]$ ,  $j = 1$  to  $J$ , of the equation

$$\frac{\varpi}{2} \sum_{n=0}^{\infty} \int_{-1}^1 (2n+1) g^n \frac{g_n(\mu) P_n(\mu)}{\nu - \mu} d\mu - 1 = 0. \quad (21)$$

The polynomials<sup>18</sup>  $g_n(\nu)$  can be defined by

$$g_n(\nu) = \int_{-1}^1 P_n(\mu) \phi(\nu, \mu) d\mu \quad (22)$$

and can be computed with the recursion relation

$$(2n+1)(1 - \varpi g^n) \nu g_n(\nu) = (n+1) g_{n+1}(\nu) + n g_{n-1}(\nu) \quad (23)$$

with starting values  $g_0(\nu) = 1$  and  $g_1(\nu) = (1 - \varpi)\nu$ . In practice it is best to use the largest eigenvalue in Eq. (18).

Once the beam attenuation coefficient  $c$  has been determined from Eqs. (17) and (18), then, with the value of  $\varpi$  already estimated, the absorption and scattering coefficients follow from

$$a = (1 - \varpi)c, \quad (24)$$

$$b = \varpi c. \quad (25)$$

## C. Determination of the Backscattering Coefficient

To compute  $b_b/b$  of Eq. (2) from the estimated values of  $\varpi$ ,  $b$ , and  $g$ , we use an equation from van de Hulst<sup>19</sup> or from Mobley *et al.*<sup>9</sup> for the HG phase function:

$$\frac{b_b}{b} = \frac{1-g}{2g} \left[ \frac{1-g}{(1+g)^{1/2}} - 1 \right]. \quad (26)$$

#### D. Determination of the Bottom Reflectance

We assume that the bottom reflects radiance with albedo  $\rho$  according to the specular–diffuse boundary condition:

$$L(\tau_*, -\mu) = \rho \left[ (1 - \gamma)L(\tau_*, \mu) + 2\gamma \times \int_0^1 \mu' L(\tau_*, \mu') d\mu' \right], \quad 0 \leq \mu \leq 1, \quad (27)$$

where  $\gamma$  is the fraction of the reflected radiance that is Lambertian. The data for  $L(\tau_2, \mu)$  in Eqs. (5) and (6) now are assumed to be from  $\tau_2 \approx \tau_*$  so that Eq. (27) can be used. (In practice, measurements at a third, independent depth,  $\tau_3 \geq \tau_2$  and  $\tau_3 \approx \tau_*$ , make the results better.) Use of Eq. (27) in Eqs. (7)–(11) yields

$$E_n(\tau_2) = (-1)^n [\rho(1 - \gamma)E_n^{(h)}(\tau_2) + 2\rho\gamma\alpha_n E_1^{(h)}(\tau_2)] + E_n^{(h)}(\tau_2), \quad (28)$$

$$S(\tau_2) = \rho(1 - \gamma) \int_0^1 [L(\tau_2, \mu)]^2 d\mu + 2\rho\gamma E_0^{(h)}(\tau_2) E_1^{(h)}(\tau_2), \quad (29)$$

$$\tilde{E}_n(\tau_2) = (-1)^{n+1} [\rho(1 - \gamma)\tilde{E}_n^{(h)}(\tau_2) + 2\rho\gamma\tilde{\alpha}_n \tilde{E}_1^{(h)}(\tau_2)] + \tilde{E}_n^{(h)}(\tau_2), \quad (30)$$

$$\tilde{S}(\tau_2) = \rho(1 - \gamma) \int_0^1 [\mu L(\tau_2, \mu)]^2 d\mu + \frac{2}{3} \rho\gamma E_1^{(h)}(\tau_2) \times [2E_2^{(h)}(\tau_2) + E_0^{(h)}(\tau_2)], \quad (31)$$

where the half-range moments are

$$E_n^{(h)}(\tau_2) = \int_0^1 P_n(\mu)L(\tau_2, \mu)d\mu, \quad (32)$$

$$\tilde{E}_n^{(h)}(\tau_2) = \int_0^1 \mu P_n(\mu)L(\tau_2, \mu)d\mu, \quad (33)$$

$$\alpha_n = \int_0^1 P_n(\mu)d\mu, \quad (34)$$

$$\tilde{\alpha}_n = \int_0^1 \mu P_n(\mu)d\mu. \quad (35)$$

Subsequent use of Eqs. (28) and (29) in Eq. (5) and use of Eqs. (30) and (31) in Eq. (6) yield a pair of equations for  $\rho$  and  $\gamma$  that can be solved to determine these parameters. Only Eq. (5) or (6) is needed if there is no specular reflection.

### 3. Numerical Tests with General Equations

We test the procedure with numerically simulated data generated from Hydrolight<sup>8</sup> to determine  $g$  and

**Table 1. Benchmark Tests of Eqs. (5) and (6) for Radiance Measurements Computed from Hydrolight with  $g = 0.9$ ,  $\varpi = 0.5$ ,  $n = 1$ , and with the Sun in a Black Sky**

Quads	% Error in $g$	% Error in $\varpi$
20	2.2	1.5
100	0.1	0.1
300	0.05	0.06

$\varpi$  with measurements at one depth and two depths. In the latter case we also can determine  $\Delta\tau$  from which we obtain  $a$ ,  $b$ , and  $b_b$ . If measurements are made at a third depth close to the bottom, then we can also estimate  $\rho$  and  $\gamma$ .

We initially test the effects of the number of Hydrolight quads used in the polar angle measurement. This is done both with the idealized case of no index of refraction mismatch at the surface and no wind speed and then with these effects included. Tests also are done with the particle phase function that simulates more realistic waters with a phase function that is not monotonically decreasing as the scattering angle increases, as with the HG model.

The procedure for the tests is as follows: The value of  $g$  is first determined when we eliminate  $\varpi$  from Eqs. (5) and (6) and solve the resulting nonlinear equation for  $g$ . The root solving routine *z Brent* from Press *et al.*<sup>20</sup> was used for this purpose. Then the value of  $\varpi$  is determined from Eq. (5). The inverse algorithm to estimate the optical thickness  $\Delta\tau$  uses the method outlined in Garcia and Siewert<sup>21</sup> to compute the Chandrasekhar polynomials and the discrete eigenvalues from Eq. (21) needed to determine  $c$  from Eqs. (17) and (18). For the tests we initially used the Hydrolight outputs as data for the inverse algorithm. Following this we introduced noise into the Hydrolight results to test the effect of measurement errors on the inverse procedure.

#### A. Initial Tests

The sensitivity of the inverse algorithm to the number of quads used in the solution procedure of Hydrolight was first evaluated. This test was run with the best conditions possible for the inverse method—the scattering was described by the HG phase function, the wind speed was zero, and the data were for only one depth just beneath the surface with the other depth assumed at  $\tau \rightarrow \infty$ . With the standard quad partitions of Hydrolight (i.e., 20 polar and 15 azimuthal quads), the recovered values of  $g$  and  $\varpi$  were within 2% of those used for the forward problem. Table 1 illustrates the effects of the number of quads on the computed values of  $g$  and  $\varpi$ . Following this test we elected to use 100 polar quads for all subsequent tests. This gave an acceptable accuracy of around 2% near the surface, thus illustrating a generic source of error with the inversion algorithm just beneath the air–water interface even if noise-free data are used. We also found that taking the measurements at larger depths reduced the errors because the effects on the light field of the index of

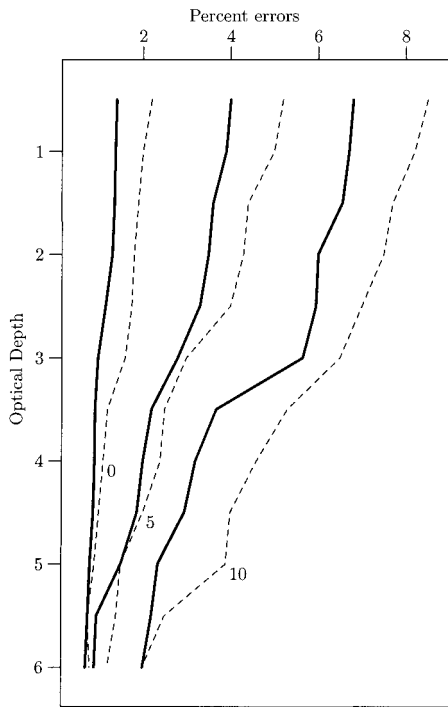


Fig. 1. Evaluation of  $g$  and  $\varpi$  for the forward problem run with the HG phase function with  $g = 0.9$ . The solid curves show the errors in  $g$ , and the dashed curves show the errors in  $\varpi$ . The numbers next to the curves show the wind speed in meters per second.

refraction mismatch at the surface diminish with depth.

With the completion of these initial tests, we performed all subsequent tests using the particle phase function<sup>22</sup> for the Hydrolight input, for which the mean cosine of scattering (the scattering asymmetry factor) was  $g = 0.923$ . We obtained the numerical results displayed assuming a black sky with a solar zenith angle of  $30^\circ$ , which gave slightly poorer results than for cases with a diffuse surface illumination.

### B. Single-Depth Algorithm Test

For this application, we determined  $g$  and  $\varpi$  from Eqs. (5) and (6) for an infinitely deep water body ( $\tau_* \rightarrow \infty$ ) using a single set of radiance data for one depth. We tested the sensitivity of the method by using various values of wind speeds in the solution of the forward problem. The results are shown in Figs. 1 and 2 for  $\varpi = 0.5$  and index of refraction  $n = 1.34$  for the forward problem input data obtained for the HG and particle phase functions, respectively. When subsurface measurements were used, for calm waters (zero wind speed) the errors in  $g$  were within 2.5% and in  $\varpi$  were within 1.5%. For higher wind speeds the errors increased up to 8.5% for a wind speed of 10 m/s. Use of data from greater depths reduced the errors to within 2% even for a 10-m/s wind-blown surface.

Noise was then added to the radiance data used as input to the inverse algorithm. The bounds of this noise were such that the  $\pm 3\sigma$  limits for the Gaussian random number generator were set to a fixed percent

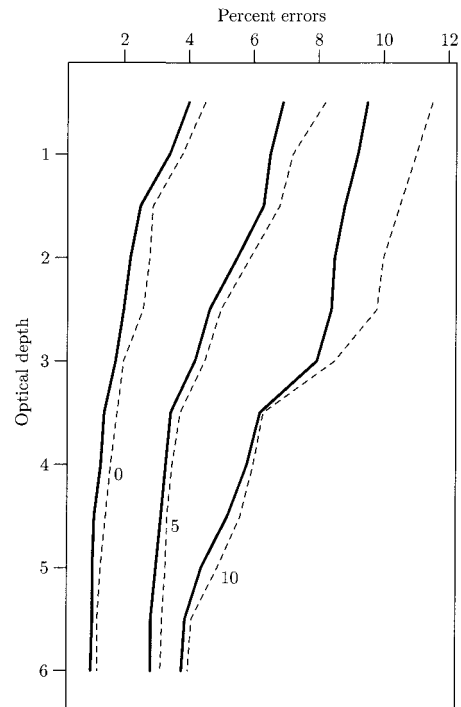


Fig. 2. Same as Fig. 1 except for the forward problem run with the particle phase function.

of the radiance value. Tests were run with various percent noise values. On adding 3% noise to the data, we retrieved the values of  $g$  and  $\varpi$  to within approximately 10% accuracy with surface wind speeds of zero. Noise of 5% increased the errors in the retrieved values of  $g$  to more than 18%. With a wind speed of 5 m/s and with 3% noise, the errors in  $g$  increased to approximately 8%. Generally, the effects of wind speed on the errors in  $g$  and  $\varpi$  diminished with data from larger depths.

### C. Two-Depth Algorithm Tests

To test the complete algorithm to evaluate  $g$ ,  $a$ ,  $b$ , and  $b_b$ , data from two depths are required. For this, in addition to using Eqs. (5) and (6), we used Eq. (18) to determine the optical thickness  $\Delta\tau$  of the water between the two measurement depths. Once that optical thickness was determined, we evaluated the beam attenuation coefficient using Eq. (17) and hence  $a$  and  $b$  using Eqs. (24) and (25). Finally, we used Eq. (26) to determine  $b_b$ . The results of the tests performed are shown in Figs. 3 and 4 for the case of  $\varpi = 0.5$  and  $n = 1.34$  for the forward problem input data obtained for infinitely deep waters with the HG and the particle phase functions, respectively. A depth difference of  $\Delta z = 4$  m was used in the algorithm.

The results show that the two-level algorithm allowed us to calculate the values of  $a$  and  $c$  with errors to within 2.5% for the case of calm waters using subsurface measurements. For these waters the value of  $b_b$  was retrieved with an error of 3.2%. Increasing the wind speed increased the errors in the calculated

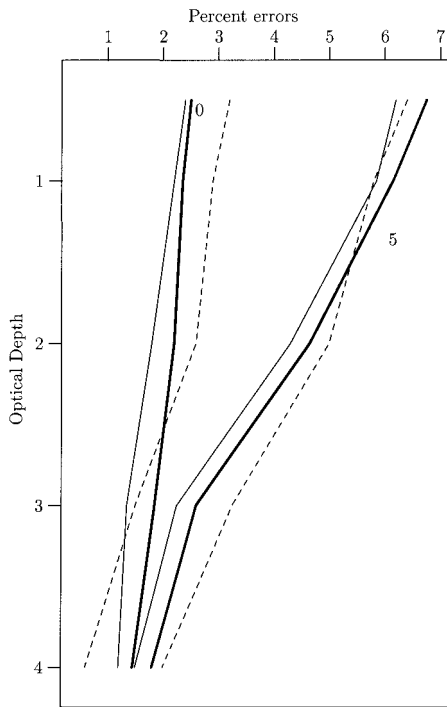


Fig. 3. Evaluation of  $\varpi$ ,  $c$ , and  $b_b$  for the forward problem run with the HG phase function with  $g = 0.9$ . A depth difference of  $\Delta z = 4$  m was used in the inverse algorithm. The heavy solid curves show the errors in  $c$ , the thin solid curves show the errors in  $\varpi$ , and the dashed curves show the errors in  $b_b$ . The numbers next to the curves show the wind speed in meters per second.

values, as expected. Also, as observed above, the errors diminished if the two measurement locations were assumed to be made at deeper depths.

For noise up to 3% the algorithm was stable, and the retrieved values of  $a$  and  $c$  were evaluated to within 10%.

#### D. Three-Depth Algorithm Tests

To test the algorithm for waters of finite depth, data from two depths are first used to obtain the water IOPs, and then data from a third depth near the bottom allow us to calculate the bottom reflectance properties. To evaluate the bottom reflectance, Hydrolight runs for a shallow water body of 5 m in depth were used to obtain radiance data at 0.5, 3.5, and 4.5 m, respectively. We determined the values of  $g$  and  $\varpi$  from Eqs. (5) and (6) using the measurements at 0.5 and 3.5 m. Equations (28)–(31) then were used in Eqs. (5) and (6) to obtain  $\rho$  and  $\gamma$  with the data from 0.5 and 4.5 m.

The results show that values of  $\rho$  were retrieved within 6.5% for the case of calm waters and to within 12% for the case of 10-m/s wind-blown surfaces. The value of  $\gamma$  was retrieved to a similar accuracy. In general it was seen that the errors increased as  $\gamma \rightarrow 0$ . The results of this test are shown in Fig. 5.

#### 4. Approximate Method

To avoid the need for the radiance measurements, can something be salvaged from this procedure to

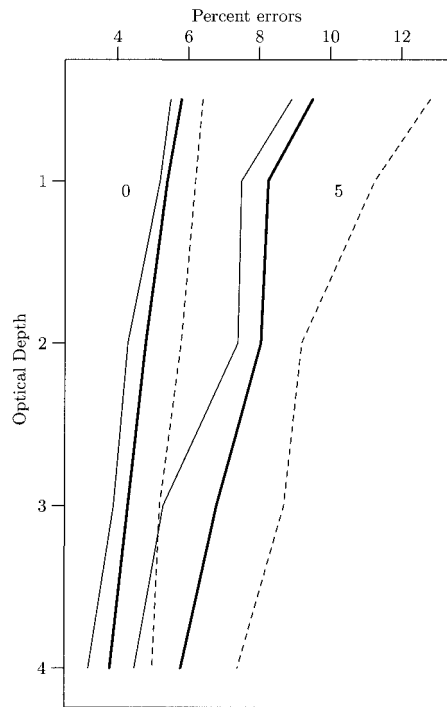


Fig. 4. Same as Fig. 3 except for the forward problem run with the particle phase function.

determine the optical properties? Specifically, can a simplified version be developed to determine  $\varpi$  and  $g$  that avoids the need for all the directional moments in Eqs. (7)–(10)? The answer is yes, but the penalty is that it must be assumed that the radiance is approximately in the asymptotic regime so that<sup>23,24</sup>

$$L(\tau, \mu) \approx A(\nu_1)\phi(\nu_1, \mu)\exp(-\tau/\nu_1) + A(-\nu_1)\phi(-\nu_1, \mu)\exp(\tau/\nu_1), \quad (36)$$

where  $\nu_1$  is the largest eigenvalue obtained from Eq. (21). [Here  $A(\nu_1)$  and  $A(-\nu_1)$  are coefficients that depend on the properties of the water and the surface

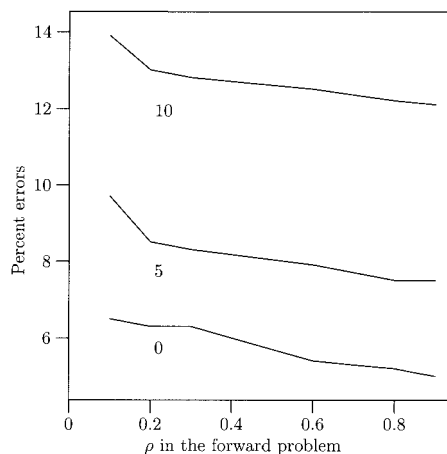


Fig. 5. Evaluation of bottom reflectivity  $\rho$  for a water column of 5 m with a Lambertian bottom. The numbers next to the curves show the wind speed in meters per second.

illumination.] After we insert approximation (36) in Eq. (7) and use Eq. (22), it follows that

$$E_n(\tau) \approx g_n(\nu_1)[A(\nu_1)\exp(-\tau/\nu_1) + (-1)^n A(-\nu_1)\exp(\tau/\nu_1)]. \quad (37)$$

Similarly it follows from Eq. (9), after use of the recursion relation for Legendre polynomials and Eq. (23), that

$$\tilde{E}_n(\tau) \approx \nu_1(1 - \varpi g^n)g_n(\nu_1)[A(\nu_1)\exp(-\tau/\nu_1) + (-1)^{n+1}A(-\nu_1)\exp(\tau/\nu_1)]. \quad (38)$$

Approximations (37) and (38) illustrate that the higher-order angular moments of the radiance can be related to lower-order ones provided that the asymptotic approximation is valid. For example,

$$E_2(\tau)/E_0(\tau) = g_2(\nu_1) = 2^{-1}[3(1 - \varpi)(1 - \varpi g)\nu_1^2 - 1]. \quad (39)$$

As a consequence of the degeneracy of the higher-order angular moments of the radiance, it has been shown that Eqs. (14) and (16) can be combined into a single equation<sup>24</sup>:

$$[\nu_1(1 - \varpi)]^2[E_0^2(\tau_2) - E_0^2(\tau_1)] = [E_1^2(\tau_2) - E_1^2(\tau_1)], \quad (40)$$

a result that also can be derived directly from a transport-corrected diffusion approximation.<sup>24</sup> Equation (40) couples together in a nonlinear way the values of the unknowns  $\varpi$  and  $g$  and involves the eigenvalue  $\nu_1$ .

The approximate method consists of our using Eqs. (21), (39), and (40) to determine the three unknowns  $\varpi$ ,  $g$ , and  $\nu_1$ . The method requires measurement of  $E_0(\tau)$ ,  $E_1(\tau)$ , and  $E_2(\tau)$ . Measurements of  $E_2(\tau)$  could be performed with the detector developed by Doss and Wells.<sup>16</sup>

To determine  $\Delta\tau$  and then  $c$ , we can no longer use Eq. (18) as it degenerates with the assumption that the radiance is asymptotic. Instead we multiply approximation (36) by  $\mu$  and integrate from  $\mu = -1$  to  $+1$  and divide the resulting relation for two different depths to obtain

$$\Delta\tau = \nu_1 \ln[E_1(\tau_1)/E_1(\tau_2)], \quad (41)$$

where we assumed that the water is infinitely deep, i.e.,  $A(-\nu_1) = 0$ .

### 5. Numerical Tests with the Approximate Method

We tested the approximate method only for the determination of  $\varpi$ ,  $g$ ,  $a$ , and  $b_b$  because the asymptotic approximation is not compatible with the need for making measurements near the bottom if the bottom reflectance properties  $\rho$  and  $\gamma$  are to be determined. To perform the tests we used Hydrolight output to determine  $E_0$ ,  $E_1$ , and  $E_2$  at various depths and used these as input in our inverse equations. We facilitated the solution to the nonlinear system by precom-

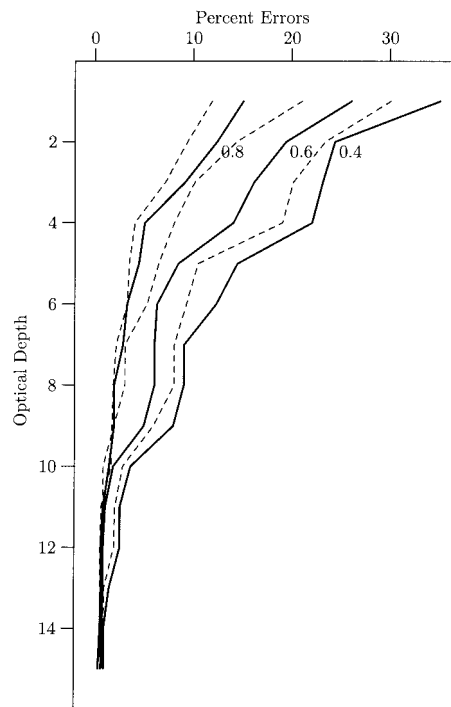


Fig. 6. Evaluation of  $g$  and  $\varpi$  with the approximate algorithm for the forward problem run with the particle phase function and no wind. The solid curves show the errors in  $g$ , and the dashed curves show the errors in  $\varpi$ . The numbers next to the curves show  $\varpi$  used in the forward problem run.

puting a two-dimensional look-up table to relate values of  $\varpi$ ,  $g$ , and  $\nu_1$  in the range  $g \in [0, 1]$  and  $\varpi \in [0, 1]$ .

The results of our tests are shown in Fig. 6 where it is clear that the errors in the retrieved values of  $g$  and  $\varpi$  decrease as irradiance measurements are taken at deeper depths. It is also clear from Fig. 6 that better approximations are obtained at shallower depths as the albedo of single scattering increases. This is consistent with the fact that the radiance approaches its asymptotic value at shallower depths as the albedo increases. Comparison of Fig. 6 with its counterpart in Fig. 2 for the radiance measurements made with no wind show that the errors with the diffusion approximation are not less than 2% until reaching  $\sim 10$  optical depths, whereas with the radiance measurements such errors occur at  $\sim 3$  optical depths.

### 6. Discussion

The single-scattering asymmetry factor  $g$  and the albedo  $\varpi$  can be determined with radiance data at one depth when the water is assumed to be infinitely deep. From data at two depths, in addition to  $g$  and  $\varpi$ , the scattering, absorption, and backscattering parameters ( $b$ ,  $a$ , and  $b_b$ ) also can be determined. If additional data at a third depth close to the bottom are available, the two parameters characterizing the specular-diffuse bottom boundary condition can be estimated.

The numerical tests performed without simulated experimental noise showed for the particle and HG

phase functions that the values of  $g$ ,  $\omega$ , and  $\Delta\tau$  could be predicted to within 2% accuracy for calm waters and to within 8–10% for wind-blown waters. The bottom reflectance properties could be predicted to within 7–12% depending on the surface wind speed.

The effect of experimental noise also was simulated. It was seen that the algorithm performed well with 3% noise. Increasing the noise beyond this value degraded the retrieved IOPs and bottom reflectance parameters. In some cases the root finding routine returned multiple values of  $g$ , hence demonstrating that the inverse problem with noisy data is nonunique.

If the radiance is assumed to be asymptotic, then the need to make full radiance measurements is eliminated and only the scalar and planar irradiance and a third irradiance are needed for the inversion. The numerical tests performed show that the approximate algorithm can be used to determine  $g$ ,  $\omega$ ,  $b$ ,  $a$ , and  $b_b$  with sufficient accuracy as long as the measurements are made at large depths.

This research was supported by the U.S. Office of Naval Research. We appreciate helpful discussions with R. Sanchez and C. D. Mobley.

## References

1. C. D. Mobley, *Light and Water. Radiative Transfer in Natural Waters* (Academic, New York, 1994), pp. 157–165 and 281 ff.
2. H. R. Gordon and G. C. Boynton, "Radiance–irradiance inversion algorithm for estimating the absorption and backscattering coefficients of natural waters: homogeneous waters," *Appl. Opt.* **36**, 2636–2641 (1997).
3. R. A. Leathers and N. J. McCormick, "Ocean inherent optical property estimation from irradiances," *Appl. Opt.* **36**, 8685–8698 (1997).
4. H. R. Gordon and G. C. Boynton, "Radiance–irradiance inversion algorithm for estimating the absorption and backscattering coefficients of natural waters: vertically stratified water bodies," *Appl. Opt.* **37**, 3886–3896 (1998).
5. R. A. Leathers, C. S. Roesler, and N. J. McCormick, "Ocean inherent optical property determination from in-water light field measurements," *Appl. Opt.* **38**, 5096–5103 (1999).
6. E. S. Chalhoub and H. F. Campos Velho, "Simultaneous estimation of radiation phase function and albedo in natural waters," *J. Quant. Spectrosc. Radiat. Transfer* **69**, 137–149 (2001).
7. L. C. Henyey and J. L. Greenstein, "Diffuse radiation in the galaxy," *Astrophys. J.* **93**, 70–83 (1941).
8. C. D. Mobley, Hydrolight software program, available from Sequoia Scientific, Inc., Westpark Technical Center, 15317 NE 90th St., Redmond, Wash. 98052.
9. C. D. Mobley, L. K. Sundman, and E. Boss, "Phase function effects on oceanic light fields," *Appl. Opt.* **41**, 1035–1050 (2002).
10. K. J. Voss and G. Zibordi, "Radiometric and geometric calibration of a visible spectral electrooptic 'fisheye' camera radiance distribution system," *J. Atmos. Oceanic Technol.* **6**, 652–662 (1989).
11. K. J. Voss, "Use of the radiance distribution to measure the optical absorption coefficient in the ocean," *Limnol. Oceanogr.* **34**, 1614–1622 (1989).
12. K. J. Voss and A. L. Chapin, "Measurement of the point spread function in the ocean," *Appl. Opt.* **29**, 3638–3642 (1990).
13. K. J. Voss and Y. Liu, "Polarized radiance distribution measurements of skylight. I. System description and characterization," *Appl. Opt.* **36**, 6083–6094 (1997).
14. R. A. Leathers and N. J. McCormick, "Algorithms for ocean-bottom albedo determination from in-water natural-light measurements," *Appl. Opt.* **38**, 3199–3205 (1999).
15. C. E. Siewert, "Inverse solutions to radiative-transfer problems based on the binomial or the Henyey-Greenstein scattering law," *J. Quant. Spectrosc. Radiat. Transfer* **72**, 827–835 (2002).
16. W. Doss and W. H. Wells, "Undersea compound radiometer," *Appl. Opt.* **22**, 2313–2321 (1983).
17. N. J. McCormick, "Transport scattering coefficients from reflection and transmission measurements," *J. Math. Phys.* **20**, 1504–1507 (1979).
18. S. Chandrasekhar, *Radiative Transfer* (Dover, New York, 1960), Sect. 48.3.
19. H. C. van de Hulst, *Multiple Light Scattering* (Academic, New York, 1980), Vol. 2, p. 307.
20. W. H. Press, S. A. Teukolsky, W. T. Vetterling, and B. P. Flannery, *Numerical Recipes in C* (Cambridge U. Press, Cambridge, UK, 1997), Chap. 9.
21. R. D. M. Garcia and C. E. Siewert, "On computing the Chandrasekhar polynomials in high order and high degree," *J. Quant. Spectrosc. Radiat. Transfer* **43**, 201–205 (1990).
22. T. J. Petzold, "Volume scattering functions for selected ocean waters," SIO Ref. 71–78 (Scripps Institution of Oceanography, San Diego, Calif., 1972).
23. N. J. McCormick, "Asymptotic optical attenuation," *Limnol. Oceanogr.* **37**, 1570–1578 (1992).
24. N. J. McCormick, "Methods for estimating the similarity parameter of clouds from internal measurements of the scattered radiation field," *J. Quant. Spectrosc. Radiat. Transfer* **33**, 63–70 (1985).